

Preliminary Analysis on Vibration Problems of Submerged Floating Tunnel and Model Test Design



Heng Lin , Yiqiang Xiang , Zhengyang Chen , and Bing Bai 

Abstract Submerged floating tunnel (SFT) is a novel type of cross-sea traffic structure, which is different from the traditional bridge and immersed tunnel. With the help of its own buoyancy to balance the operational loads, SFT shows great potential for crossing long, large, and deep waterways. Since floating in the underwater environment all year around, SFT has to face a series of vibration problems during the operation. In this paper, some vibration problems of SFT, such as wave-induced vibration, vortex-induced vibration, vibration caused by accidental loading, and vehicle-induced vibration, are summarized. In the meantime, combined with the features of SFT, the test model is designed and manufactured in the work. The geometric scale ratio of the whole model is about 1:100. Some aluminum tubes, connected by the flanges, are used for simulating the main body of SFT. Two plexiglass boxes provide the platform for the model test car to move in the aluminum tubes. The cable force, displacement, and acceleration at the points in the control sections of the tube are monitored during the model test. The whole experimental work provides a meaningful reference and solid foundation for further study on vibration problems of SFT.

Keywords Submerged floating tunnel · Model design · Fluid-vehicle-tunnel interaction · Experimental study

H. Lin (✉) · Y. Xiang · Z. Chen · B. Bai
Department of Civil Engineering, Zhejiang University, Hangzhou, China
e-mail: linh@zju.edu.cn

Y. Xiang
e-mail: xiangyiq@zju.edu.cn

Research Center for Submerged Floating Tunnel, CCEA, ZJU, Hangzhou, China

1 Introduction

Since the beginning of the twenty-first century, China's economy has gradually developed from a single land economy to a model of common development of land, sea, and island construction. Making some coastal developed cities and islands with rich resources to form strong economic circles and belts has become one of the important measures for China's economic growth and development engine. In such a times background, submerged floating tunnel (SFT) has been proposed for crossing long and deep waterways and connecting the strait sides [1]. It is generally composed of tunnel tubes suspended in water, anchor cables limiting displacement of tunnel, deep water foundations and revetments connecting quayside, as shown in Fig. 1. Compared to available strait-crossing techniques, such as bridges, immersed or undersea tunnels, the SFT has many advantages in the construction cost and great spanning ability. Besides, due to lower environmental impact, less sensitivity to windstorm and thunder actions, the SFT has raised lots of researchers' and engineer's attention.

Due to complex submarine topography and geological conditions, it makes the behavior of submerged floating tunnel and analysis to be very complicated. Kunisu et al. adopted the boundary element method (BEM) and Morison equation to study the wave force characteristics acting on the SFT. The results of Morison equation and BEM showed a great agreement [2]. Li et al. deduced an analytical equation on lock-in velocity of the tether under the influence of vortex-excited vibration [3]. Mai et al. focused on the VIV of the tether and researched the transverse vortex-induced response of the tether installed on the tube [4]. Taking a section of the SFT as a study object, Ge et al. derived the tube-tether coupled vibration equations by Hamilton variation principle [5]. Xiang et al. [6] refined the assumptions and established the tube-tether coupled vibration model considering the boundary constraint. The results show the initial disturbance of the SFT tube has a greater influence on the instantaneous amplitude of the tethers and the coupling effect of tube-tether vibration will be weaker with a smaller tether inclined angle. Besides, by both considering the fluid-structure and the soil-structure interaction, Fogazzi et al. [7] developed a nonlinear numerical analysis procedure for a seabed anchored floating

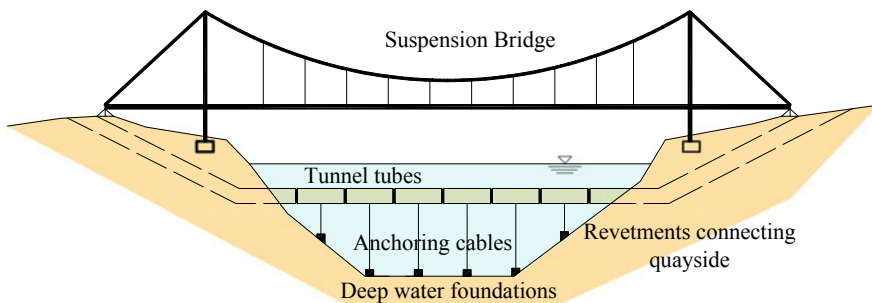


Fig. 1 Typical submerged floating tunnel and suspension bridge

tunnels under extreme seismic excitation. Di Pilato et al. [8] refined the geometrically nonlinear finite element and established a full 3D model for the response of the Messina Strait crossing due to seismic and wave loads. SFT as a future marine transportation structure, these studies lay the firm foundation for the SFT design and construction.

Up to now, there is no practice project of the SFT in the world. So the model test becomes one of the effective means to validate the theoretical analysis method. In 1994, Yoshihara et al. placed the models in a circulating water channel horizontally and normal to the direction of current flow, and investigated the VIV of the tube [9]. Seo et al. [10] did the physical models test in a wave flume for verifying the hydrodynamic forces theoretical calculation method. A LED target was placed on the bar above the SFT model to record the displacement of SFT. A simple slack condition was captured during the experimental test and should be avoided. To control VIV of the tether in the acceptable range, Chao et al. [11] studied the effect of three different disturbing flow devices by the experiments. The results show the spiral fringe has the greatest effect in all working conditions. According to the existed references, most of the model tests take a segment of the SFT as the study object. It ignores the effect of revetments connecting, which may amplify the test results. This paper summarizes the vibration problems in the SFT and takes the vehicle-tunnel coupled model test as an example to illustrate.

2 Requirements of the SFT Experimental Model

2.1 Similarity Requirements

Due to the limitation of the test site and equipment, it is usually to scale the structure to a certain size in the process of model test design. Similitude model and scaled model are two typical methods commonly used in structural experiment design. Similitude models generally require geometric similarity, kinematic similarity, and material similarity. When all similar conditions are met, the behavior of the real structure under loading can be monitored from the similitude model. However, the similarity requirements of the scaled model are relatively less stringent. The model test is generally used for verifying the theoretical calculation method and analyzing the parametric influence.

Like other offshore structures, the SFT operates under the water and is affected by the external fluid environment. In order to simulate the fluid-structure interaction between the real structures, the fluid similarity and the structural similarity are needed in the model test. The flow of incompressible viscous fluid is controlled by the Navier–Stokes equations and the continuity equations [12].

$$\text{The Navier-Stokes equations: } \frac{\partial v_i}{\partial t} + v_j \frac{\partial v_i}{\partial x_j} = f_i - \frac{1}{\rho_w} \frac{\partial p}{\partial x_i} + \nu \nabla^2 v_i \quad (1)$$

$$\text{The continuity equations: } \frac{\partial v_i}{\partial x_i} = 0 \quad (2)$$

in which v_i is flow velocity; ρ_w is fluid density; p is the fluid pressure; ν is dynamic viscosity of the fluid; t is time; f_i is specified body-force; x_i is Cartesian coordinate; the range of the index of i denotes 1, 2, 3 for three-dimensional applications. In the model test design, the scale ratios of the physical parameters are carried out to quantitatively describe the similarity relation. According to the Navier–Stokes equations and continuity equations, the similarity relations between real fluid field and the test can be written as

$$\frac{\lambda_v}{\lambda_t} = \frac{\lambda_v^2}{\lambda_l} = \lambda_g = \frac{\lambda_p}{\lambda_{\rho_w} \lambda_l} = \frac{\lambda_v \lambda_v}{\lambda_t^2} \quad (3)$$

where λ is scale ratio of the physical parameter; the subscripts “ v ”, “ t ”, “ l ”, “ g ”, “ p ”, “ ρ_w ”, and “ ν ” denote the basic parameters mentioned in Eqs. (1) and (2). Further processing of Eq. (3), hydrodynamic parameters, such as Strouhal number, Reynolds number, Froude number, and Euler number, can be acquired.

$$\begin{aligned} \text{Strouhal number: } \lambda_l / \lambda_t \lambda_v &= 1; \text{ Reynolds number: } \lambda_l \lambda_v / \lambda_\nu = 1; \\ \text{Froude Number: } \lambda_v^2 / \lambda_g \lambda_l &= 1; \text{ Euler number: } \lambda_p / \lambda_\rho \lambda_v^2 = 1; \end{aligned} \quad (4)$$

The state of the structure can be determined by the equilibrium equations, constitutive equations, strain–displacement relations, and boundary conditions [13].

$$\text{The equilibrium equations: } \frac{\partial \sigma_{ij}}{\partial x_i} + f_i = \rho_s \frac{\partial u_i}{\partial t^2} \quad (5)$$

$$\text{The constitutive equations: } \sigma_{ij} = \lambda_s \delta_{ij} \varepsilon_{kk} + 2\mu_s \varepsilon_{ij} \quad (6)$$

$$\text{The strain-displacement relations: } \varepsilon_{ij} = \frac{1}{2} \left(\frac{\partial u_i}{\partial x_j} + \frac{\partial u_j}{\partial x_i} \right) \quad (7)$$

$$\text{The boundary conditions: } \bar{\Gamma}_i^\sigma = \sigma_{ij} n_j \quad \text{and} \quad u_i = \bar{u}_i \quad (8)$$

where σ_{ij} are components of stress; ε_{ij} are components of strain; ρ_s is mass density; f_i are body force components; λ_s and μ_s are Lamé elastic parameters; $\bar{\Gamma}_i^\sigma$ denotes the specified stress boundary conditions; \bar{u}_i denotes the specified displacement boundary; δ_{ij} is the Kronecker delta function; n_j is normal vector of the boundary. In the model test design, the scale ratios of the physical parameter are substituted into Eqs. (5)–(8). The similarity relations can be acquired,

$$\frac{\lambda_\sigma}{\lambda_l} = \lambda_g \lambda_{\rho_s} = \frac{\lambda_{\rho_s} \lambda_l}{\lambda_t^2} \quad \text{and} \quad \lambda_\sigma = \lambda_E \lambda_\varepsilon = \lambda_\mu \quad (9)$$

where λ is scale ratio of the physical parameter; the subscripts “ σ ”, “ l ”, “ ρ_s ”, “ E ”, “ μ ”, and “ t ” denote the physical parameters of stress, length, density, elastic modulus, Poisson’s coefficient, and time, respectively. For linear isotropic materials, λ_e is equal to 1. Besides, most materials have similar Poisson coefficients, thus λ_μ is equal to 1. So the relation, $\lambda_E = \lambda_\sigma$, can be approximately acquired.

The fluid similarity requires the four hydrodynamic parameters to be equal to 1, but it is hard to achieve unless changing the medium of the fluid ($\lambda_v = 1$). In the gravity field ($\lambda_g = 1$), the similarity of Froude number is controlled and Reynolds number is adjusted to simulate the similarity of the fluid field. At the same time, the fluid similarity limits some parameters in Eq. (9), like $\lambda_{\rho_s} = 1$ and $\lambda_E = \lambda_l$. By adding some additional mass blocks to the test model, the material density scale ratio can be satisfied. However, it is hard to find a kind of material that can satisfy the relation between the elastic modulus scale ratio and the length scale ratio. In the engineering test model design, it usually increases the thickness of the structural section to let the stiffness scale ratio to be equal to the length scale ratio of the structure ($\lambda_{EI} = \lambda_l$).

2.2 Theoretical Method of the SFT Vehicle-Tunnel Coupled Vibration

With the popularization of high-speed rail and light rail technologies, it is particularly important to analyze the dynamic behavior of the structures suffering from moving vehicle loads. Because the SFT operates in the water environment, the structure may experience some potential risks when the vehicle travels through it. Tariverdilo et al. [14] once analyzed the vibration of the SFT subjected to moving loads by establishing 2D and 3D structural models. According to the results, they conclude that the fluid-structure interaction is the reason for the magnification of the tunnel deflection. Zhang et al. [15] analyzed the dynamic behavior of the SFT under a single moving load and discussed the influence of structural design parameters. On this basis, Lin et al. [16] established the theoretical coupled model considering the fluid-vehicle-tunnel interaction. The ocean current effect is considered as a combination of lift force, inertial force, and hydraulic resistance directly acting on the SFT. Those works lay the foundation for the SFT further study (Fig. 2).

The motion governing equations of the SFT fluid-vehicle-tunnel coupled vibration can be represented as:

$$m \frac{\partial^2 w}{\partial t^2} + c \frac{\partial w}{\partial t} + EI \frac{\partial^4 w}{\partial x^4} + kw = f_v(x, t) + f_D(x, t) \tag{10}$$

where $w(z, t)$ denotes the vertical displacement of the tunnel measured from its static equilibrium position; m , c , and EI are the mass, damping, and flexural rigidity of the SFT, respectively; $f_v(x, t)$ is the moving traffic loading; $f_D(x, t)$ is the fluid loading; and k is the equivalent linear stiffness of the elastic foundation, $k = K/h$.

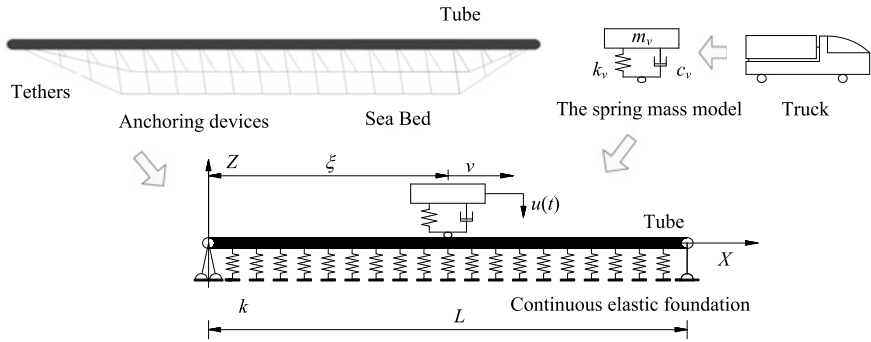


Fig. 2 Analysis model of the SFT under action of moving vehicle load

Considering the fluid-vehicle-tunnel interaction, the moving traffic loading is simply modeled as a lumped mass supported by a spring and dashpot. Based on d’Alembert’s principle, the moving loading can be written as

$$\begin{cases} f_v(x, t) = m_v g + k_v[u(t) - w(x, t)\delta(x - vt)] + c_v\left[\dot{u}(t) - \frac{\partial w(x, t)}{\partial t}\delta(x - vt)\right]; & \text{for } 0 \leq vt \leq L \\ m_v \ddot{u}(t) + k_v[u(t) - w(x, t)\delta(x - vt)] + c_v\left[\dot{u}(t) - \frac{\partial w(x, t)}{\partial t}\delta(x - vt)\right] = 0; & \text{for } 0 \leq vt \leq L \end{cases} \quad (11)$$

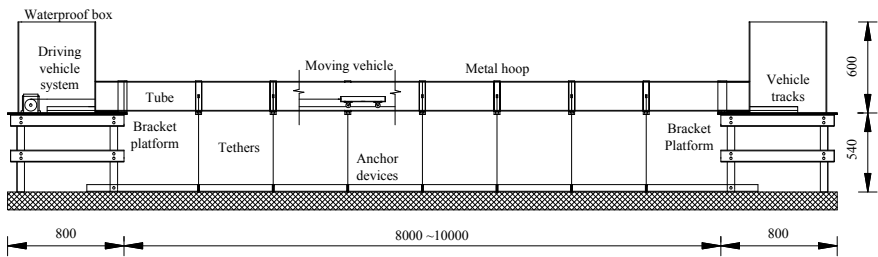
where $u(t)$ is the vertical displacement of the vehicle measured from its static equilibrium position; m_v , k_v , and c_v are the mass, stiffness, and damping of the vehicle, respectively; $\delta(\cdot)$ is Dirac’s delta function; and $\dot{(\cdot)}$ denotes derivation with respect to time.

The SFT will vibrate during the operational stage due to the traffic moving loads caused by cars or trains. Compared with the extreme loads, the magnitude of the vehicle load is not large. But the long-term periodic loads will result in the impact and fatigue-related structural damage. In the meantime, the moving vehicle also may lead to the resonance between vehicle and structure, which means that the dynamic responses of the SFT and vehicle are significantly amplified. The driving safety and comfort will be definitely affected by the resonance phenomenon. At present, the research about the fluid-vehicle-tunnel coupled vibration of the SFT is still in the initial stage; the above analysis and study have not been verified by the relative experiment. In order to understand the dynamic behavior of the SFT under the action of the moving load, it is necessary to further improve the analysis method of fluid-vehicle-tunnel interaction for the SFT and confirm the accuracy of the proposed method by the actual experimental model and test.

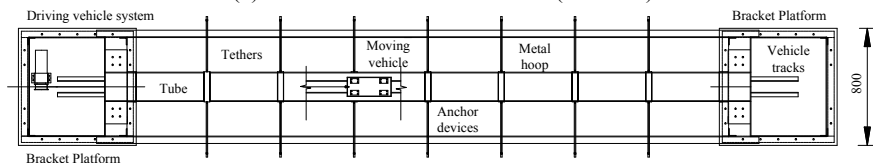
3 Design Details of the SFT Model and Sensors Arrangements

3.1 Model Design

To study the effect of the driving vehicle on the SFT under water environment, a scaled model of the SFT subjected to moving vehicle load is designed. The total SFT model is composed of the bracket platforms, the anchoring devices, the tubes, and the waterproof boxes, as shown in Fig. 3a, b. It is placed in the Stormy stream integrated sink in Ocean and Hydraulic Power Lab, Zhejiang University. The size of the test site is 65 m long and 1.2 m wide. The section height is 1.6 m, and the allowable depth of water is 1.0 m. The whole scale model is about 14 m long and 0.6 m wide. The bracket platform is made of channel steel and angle steel through bolts. The plexiglass waterproof box is fixed on the bracket platform by self-tapping screws. A circular hole with a diameter of 20 cm is reserved on one side of the waterproof box



(a) The elevation of the scale model (unit: mm)



(b) The plan of the scaled model (unit: mm)



(c) Water sink



(d) Stitching method

Fig. 3 Schematic diagram of the overall SFT model and experimental equipment

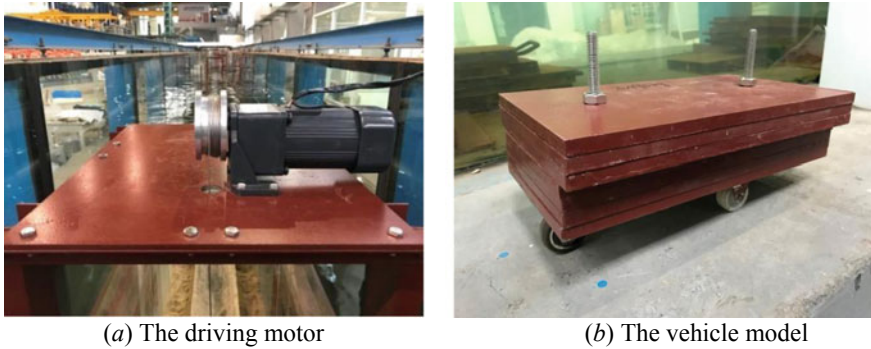


Fig. 4 The traction system and the vehicle loaded to simulate different loads

for the tube splicing. Figure 3c, d shows the experimental water sink and some details about the scaled model in reality. Meanwhile, to ensure the waterproof performance, 2 mm thick waterproof glue is applied for sealing treatment.

In the model test, the vehicle loading is controlled by the traction system and the weight of the vehicle can be adjusted by the load plates. When the traction system is working, the vehicle model drives from one side of the waterproof box to the other side. The whole process realizes the traveling process of the vehicle in the SFT. The traction system consists of a variable speed motor and frequency converter. The power of the motor should meet the requirements of the model test. The entire vehicle model is approximately rigid. Several pieces of steel plate are fixed by the front and rear bolts without falling off. The experimental vehicle loaded to simulate different loads and the driving system are shown in Fig. 4a, b.

3.2 Sensors Arrangement in the Model Test

The main object of the model test is to obtain the displacement and the acceleration at the points in the control sections of the SFT and relative forces of the anchor cables under the action of the traveling vehicle. Therefore, the sensors should be selected in terms of their sensitivity, response characteristics, linear measure range, stability, accuracy, and signal output requirements. In the model test, some uniaxial acceleration sensors are installed at the position of the $1/4L$, $1/2L$, $3/5L$, and $3/4L$, and so on control sections of the tube in the vertical direction. Meanwhile, some uniaxial displacement sensors are placed at the position of the $1/4L$, $1/2L$, $3/5L$, and $3/4L$, and so on control sections of the tube in the vertical direction. To monitor the torsion displacement of the tube under moving vehicle load, two displacement sensors are symmetrically installed on both sides of the tube in the middle span section. Cable force is measured by the force sensor setting on the tether. Because the data collection works in the water, the sensors need to be checked again to confirm

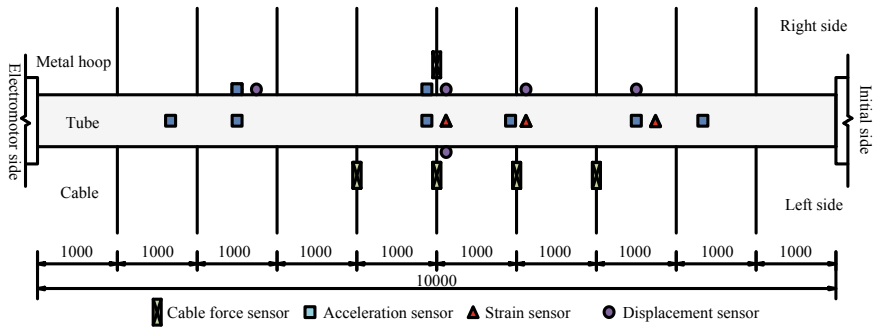


Fig. 5 The layout of sensors on the SFT model

their good working condition after each measurement starts. The layout of sensors on the SFT model is shown in Fig. 5.

3.3 Material Parameters and Test Working Cases

Because no SFT has been built anywhere in the world, the prototype parameters of the SFT take some literature as reference. Due to material properties, it is hard to realize the similitude model for the whole structure status monitoring. Considering the limitation of the test site, the geometrical scale ratio of the whole test model is set as 1:100 to analyze the driving vehicle effect on the SFT under water environment. The proportional relations of basic parameters are listed in Table 1.

Meanwhile, the dynamic model test program of the SFT is carried out in various working cases, such as the free vibration of the SFT model in the environment with and without water to acquire basic characteristics of the model, the dynamic behavior

Table 1 The proportional relations of basic parameters

Item	Prototype parameters	Scaled parameters	Scale ratio
Out diameter	20 m	0.2 m	100:1
Wall thickness	0.5 m	0.005 m	100:1
Span of the tube	1000 m	10 m	100:1
Density of the tube	2500 kg m ⁻³ (concrete)	2700 kg m ⁻³ (aluminum)	0.925:1
Elastic modulus	3.55 × 10 ⁴ MPa	7 × 10 ⁴ MPa	0.507:1
Diameter of tethers	0.5 m	0.005 m	100:1
Inclination angle	π/3	π/3	1:1
Moving vehicle load	1.2 × 10 ⁵ kg	40 kg	3000:1
Moving velocity	25 m/s	0.25 m/s	100:1
Fluid medium	1000 kg m ⁻³	1000 kg m ⁻³	1:1

of the SFT model under the moving loads to understand the effect of the traveling vehicle.

4 Test Results and Preliminary Analysis

Figure 6 shows the vertical acceleration curves of the SFT at the mid-span position in the case of the environment with and without water. It can be easily found that the amplitude of the free vibration attenuates much slower in the no water environment than in the case of the water environment. The fast Fourier transform (FFT) is used for dealing with the acceleration signals. The natural frequencies of the structure in the water environment and the no water environment are 5.280 and 2.747 Hz, respectively. The damping ratio of the structure can be acquired by the time-domain attenuation method. The damping ratio values of the structure in the environment with and without water are 0.0271 and 0.1457, respectively.

It can be seen that the vibration characteristics of the SFT in the environment with and without water show a large difference. The natural vibration frequency of the structure in the water environment reduces about 1.92 times and the damping ratio of the structure increases about 5.38 times, which verifies the influence of additional mass and fluid damping force on the structural vibration in the water environment (Fig. 7).

Besides, the deflections at the different measure positions along longitudinal direction of SFT model are recorded, as shown in Fig. 8. The dynamic amplification

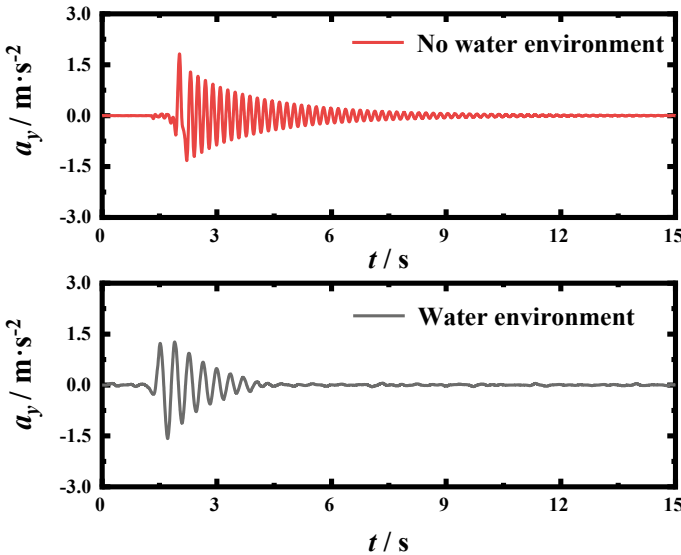


Fig. 6 Acceleration of the free vibration in the mid-span

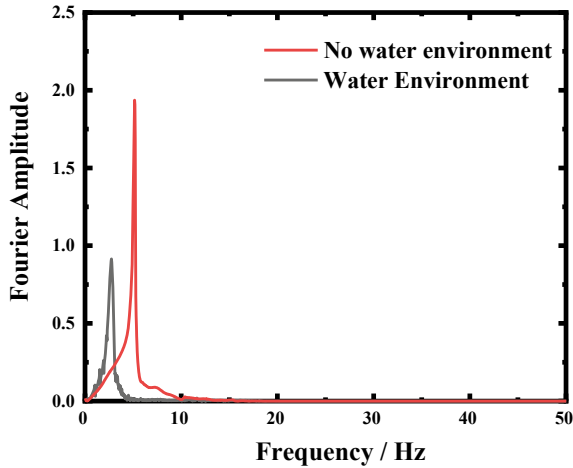


Fig. 7 Frequency spectrogram of corresponding acceleration

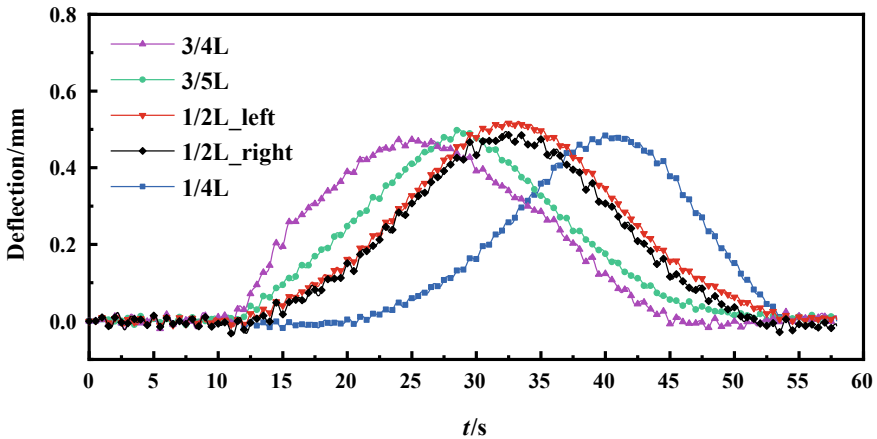


Fig. 8 The vertical deflections at the different positions of the SFT model due to the moving vehicle load

phenomenon can be observed from the results. The deflection curve shakes during the vehicle moving on the SFT. The maximum deflection value of the SFT occurs on the 1/2L_right position and is 0.521 mm. It is a little higher than the deflection of the SFT on the 1/2_left. The 1/4L and the 3/4L positions have 0.485 and 0.473 mm maximum deflection. The results show the dynamic displacement of the SFT subjected to the symmetrical moving loads generally happens on the vertical plane. The SFT has no obvious spatial behavior under the action of the symmetrical moving vehicle in the static water, which means that the SFT has sufficient support strength for vehicles driving in the structure.

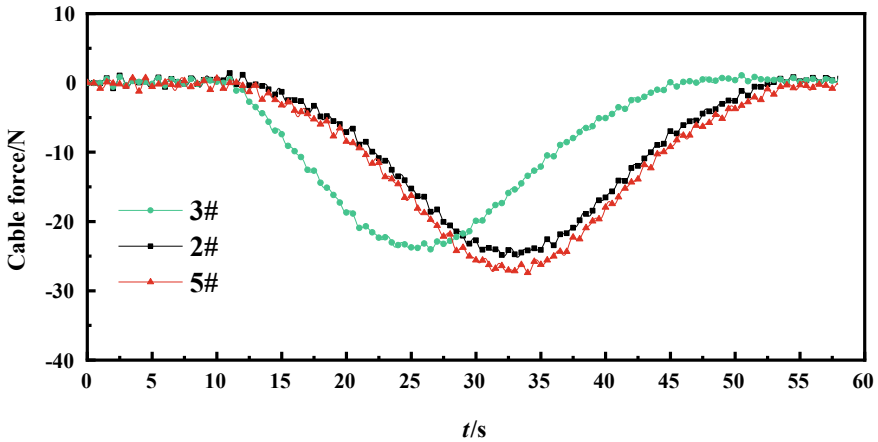


Fig. 9 Cable forces of the typical anchor cables of the SFT model due to the moving vehicle load

Meanwhile, the cable forces of the SFT on the $1/2L$ and $3/5L$ also were measured during the model experiment. The typical results of anchor cables are shown in Fig. 9. The cable force has a corresponding relationship with the deflection. The cable force of the SFT on the $1/2L_{\text{left}}$ is slightly less than that in the case of on the $1/2L_{\text{right}}$. The cable forces of the SFT are varying and then restore the original level in the process of vehicle moving. It means that the cables are in the elastic stage when the vehicle is moving on the SFT.

5 Conclusions and Prospects

As a novel underwater transport structure, the SFT receives much more attention from experts. This paper reviews some vibration problems in the SFT, such as wave-induced vibration, vortex-induced vibration, vibration caused by accidental loading, in which the vehicle-induced vibration is an inevitable problem that has been proposed these years. Meanwhile, combined with the features of SFT, the test model is designed and manufactured in the work. The cable force, displacement, and acceleration of the tube are monitored during the model test. From the test results, some conclusions can be drawn here.

1. It is difficult to design a similitude model to reflect the real SFT operating in the water. In the engineering test model design, it usually increases the thickness of the structural section to let the stiffness scale ratio equals to the length scale ratio of the structure.

2. The fluid-vehicle-tunnel coupled vibration is an important interdisciplinary research area. At present, the research about the fluid-vehicle-induced vibration in the SFT is still in the initial stage; it is necessary to consider the flow field influence in the further study.
3. From the experimental results, it is reasonable to analyze the SFT in the vertical plane when the moving vehicle acting on the SFT. Besides, the tethers are in the elastic stage when the moving vehicle acting on the SFT.

According to the phenomenon observed from the test, some further work can be carried out to study the fluid-vehicle-tunnel coupled vibration for the SFT.

Acknowledgments This work was supported by the National Natural Science Foundation of China (51541810) and (51279178).

References

1. Xiang YQ, Ying Y (2016) Challenge in design and construction of submerged floating tunnel and state-of-art. *Procedia Eng* 166:53–60. <https://doi.org/10.1016/j.proeng.2016.11.562>
2. Kunisu H (2010) Evaluation of wave force acting on submerged floating tunnels. *Procedia Eng* 4:99–105. <https://doi.org/10.1016/j.proeng.2010.08.012>
3. Li J, Li YS (2006) Analytical solution to the vortex-excited vibration of tether in the submerged floating tunnel. In: Geoshanghai international conference, pp 164–169. [https://doi.org/10.1061/40867\(199\)19](https://doi.org/10.1061/40867(199)19)
4. Mai JT, Luo ZX, Guan BS. The vortex-excited dynamic response for a submerged floating tunnel under the combined wave and current effect. *J China Railway Soc* 27(1):102–105. <https://doi.org/10.3321/j.issn:1001-8360.2005.01.020> (in Chinese)
5. Ge F, Long X, Wang L et al (2009) Study of vortex-induced vibration of submerged floating tunnel tube-tether coupled model. *China J Highw Transp* 22(3):83–88, 100. [https://doi.org/10.1016/s1874-8651\(10\)60059-2](https://doi.org/10.1016/s1874-8651(10)60059-2) (in Chinese)
6. Xiang YQ, Chao CF (2013) Vortex-induced dynamic response analysis for the submerged floating tunnel system under the effect of currents. *J Waterw Port Coast-ASCE* 139(3):183–189. [https://doi.org/10.1061/\(asce\)ww.1943-5460.0000175](https://doi.org/10.1061/(asce)ww.1943-5460.0000175)
7. Fogazzi P, Perotti F (2000) The dynamic response of seabed anchored floating tunnels under seismic excitation. *Earthq Eng Struct D* 29(3):273–295. [https://doi.org/10.1002/\(sici\)1096-9845\(200003\)29:3%3c273:aid-eqe899%3e3.0.co;2-z](https://doi.org/10.1002/(sici)1096-9845(200003)29:3%3c273:aid-eqe899%3e3.0.co;2-z)
8. Di Pilato M, Perotti F, Fogazzi P (2008) 3D dynamic response of submerged floating tunnels under seismic and hydrodynamic excitation. *Eng Struct* 30(1):268–281. <https://doi.org/10.1016/j.engstruct.2007.04.001>
9. Yoshihara S, Toyoda S, Venkataramana K et al (1996) Current-induced vibrations of submerged floating tunnels. Technical report Kagoshima University Faculty of Engineering Research Report, vol 36
10. Seo S, Sagong M, Son S (2015) Global response of submerged floating tunnel against underwater explosion. *KSCE J Civ Eng* 19(7):2029–2034. <https://doi.org/10.1007/s12205-015-0136-3>
11. Chao CF, Xiang YQ, Lin JP. Patterns of cable VIV suppression based on the fluid-structure interaction. *Mech Eng* 37(6):725–730, 718 (in Chinese)
12. Bazilevs Y, Takizawa K, Tezduyar TE (2013) Computational fluid-structure interaction: methods and applications. Wiley
13. Ziebjewicz O, Taylor R (2008) The finite element method, 4th ed. McGraw-Hill

14. Tariverdilo S, Mirzapour J, Shahmardani M et al (2011) Vibration of submerged floating tunnels due to moving loads. *Appl Math Model* 35(11):5413–5425. <https://doi.org/10.1016/j.apm.2011.04.038>
15. Zhang Y, Dong M, Ding H et al (2016) Displacement response of submerged floating tunnel tube due to single moving load. *Procedia Eng* 166:143–151. <https://doi.org/10.1016/j.proeng.2016.11.577>
16. Lin H, Xiang YQ, Yang Y et al (2018) Dynamic response analysis for submerged floating tunnel due to fluid-vehicle-tunnel interaction. *Ocean Eng* 166:290–301. <https://doi.org/10.1016/j.oceaneng.2018.08.023>